Dielectric properties of Mn doped $SrTiO_3$

2008 J. Phys.: Condens. Matter 20 095221

(http://iopscience.iop.org/0953-8984/20/9/095221)

J. Phys.: Condens. Matter **20** (2008) 095221 (6pp) doi:10.1088/0953-8984/20/9/095221

Dielectric properties of Mn doped $SrTiO_3$

M Savinov[1], V A Trepakov[1,2], P P Syrnikov[2], V Železný[1], J Pokorný[1], A Dejneka[1], L Jastrabík[1] and P Galinetto[3]

[1] Institute of Physics AS CR, Na Slovance 2, 182 21, Prague 8, Czech Republic
[2] A F Ioffe Physico-Technical Institute RAS, 194 021, St Petersburg, Russia
[3] Dipartamento di Fisica 'A Volta' Universitá di Pavia, CNISM-1-27100 Pavia, Italy

E-mail: savinov@fzu.cz

Received 21 November 2007, in final form 25 January 2008
Published 14 February 2008
Online at stacks.iop.org/JPhysCM/20/095221

Abstract

The dielectric permittivity (100 Hz–1 MHz) and IR reflectivity of $SrTiO_3$:Mn(0.1 at.%) crystals and $SrTiO_3$:Mn(0.1–3 at.%) ceramics prepared maintaining the ratio $(Sr + Mn)/Ti = 1$ or $(Ti + Mn)/Sr = 1$ (A- and B-type ceramics, respectively) were studied. Surprisingly, the magnitude and $\varepsilon'(T)$ dependence for the crystals and B-type ceramics with 0.1 at.% of Mn appeared to be nearly the same; the magnitudes rise on cooling and reach ~3000 at $T = 7$ K. At the same time, IR spectra of $SrTiO_3$:Mn(0.1 at.%) crystals reveal that TO (transverse optical) phonons yield a magnitude of low frequency permittivity of ~4000 at $T = 5$ K, evidencing crystal inhomogeneity. Both crystals, like B-type $SrTiO_3$:Mn(0.1 at.%) ceramics, reveal faint low temperature relaxations with the Arrhenius activation energies ~37–40 meV and ~120–130 meV (P- and T-relaxations). These relaxations emerge in losses only and were tentatively attributed to reorientation of defects associated with Mn^{2+}_{Ti}–O^--type polaronic centres and O^1_h–D^{18}_{4h} phase transition related effects, respectively. In reduced crystals P-relaxation strongly enhances, becoming distinctly seen in the real part of the permittivity. More heavily Mn doped A- and B-type ceramics reveal strongly pronounced Arrhenius-type dielectric relaxation with activation energy ~59–68 meV depending on the Mn concentration.

1. Introduction

Properties of Mn doped incipient ferroelectric $SrTiO_3$ (STO) have attracted extensive interest in the last few years due to improvement of practical properties of ABO_3 oxides found in STO:Mn thin films and ceramics [1, 2], magnetic ordering effects observed in Mn implanted STO crystals [3] and powder [4]. Relatively recently an intriguing low temperature dielectric relaxation has been recognized for Mn doped STO ceramics [5, 6]. This relaxation and its nature appear to be subjects of extensive studies and contradictions. It was found that STO:Mn(0.5–2 at.%) ceramics sintered with addition of MnO or MnO_2 oxides reveal similar dielectric relaxation in the 10–50 K temperature region, which obeys the Arrhenius law $\tau = \tau_0 \exp(-U/kT)$ with the high temperature relaxation time $\tau_0 \sim 5 \times 10^{-11}$ s and activation energy $U \sim 30$ meV. The nature of this relaxation was connected to reorientations of Mn^{2+}_{Ti}–O^- or O^-–Mn^{2+}_{Ti}–O^- polaronic-type related centres. However, further publications [7–10] appeared to be in serious contradiction with the data and conclusions of [5, 6]. Some authors [7–10] reported synthesis and dielectric studies of two types of $SrTiO_3$:Mn(0.5–2 at.%) ceramic compositions sintered maintaining the ratios: (i) $(Ti + Mn)/Sr = 1$ (nominated as $SrTi_{1-x}Mn_xO_3$, STM) and (ii) $(Sr + Mn)/Ti = 1$ ($Sr_{1-x}Mn_xTiO_3$, SMT). Surprisingly, STM ceramics did not reveal any dielectric relaxation at all. Mn doping reduced the magnitude of the dielectric permittivity only, driving the system away from ferroelectric instability. In contrast, a pronounced dielectric relaxation with activation energy ~86 meV (which is larger than that reported in [5, 6]) emerging in the 25–65 K region was found in SMT ceramics. Moreover, dielectric hysteresis loops have been observed in SMT ceramics too and were treated as manifestations of the phase transition to a polar phase (at $T = 85$ K for $x = 0.02$ and 60 K for $x = 0.005$). As a result it was concluded that low temperature dielectric relaxation and polar phase formation in $SrTiO_3$:Mn occur only when Mn substitutes for Sr in A-lattice positions and forms dipole reorientable Mn^{2+} off-centres. To resolve these contradictions and provide new insight into the properties and nature of low temperature dielectric relaxation in $SrTiO_3$:Mn new detailed studies are necessary. It should be mentioned that suggestions regarding the character of Mn incorporation and relaxation nature were based on studies of ceramic specimens only, in which inhomogeneity, granular

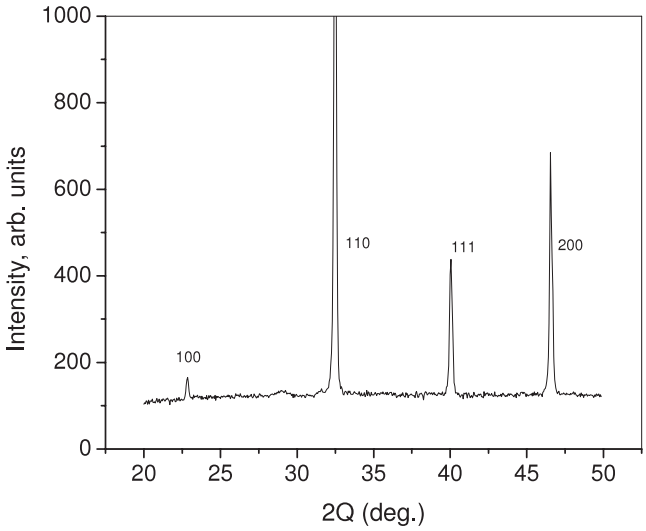

Figure 1. XRD profiles of $SrTiO_3$:Mn(0.1 at.%) B-type ceramics.

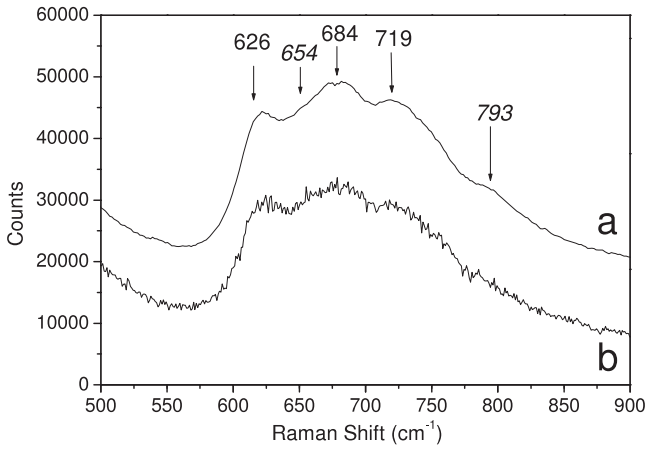

Figure 2. Raman spectra at room temperature for $SrTiO_3$:Mn(0.1 at.%) B-type ceramics (a) and $SrTiO_3$:Mn(0.1 at.%) crystals (b).

structure, grain boundary contributions can play an important role. In this regard comparative studies of dielectric properties and IR spectra of Mn doped $SrTiO_3$ crystals and ceramics are of special interest and such investigations are reported on in this paper. To our knowledge dielectric properties of $SrTiO_3$:Mn crystals have not been reported up to now.

2. Experimental details

Weakly concentrated STO:Mn(0.1 at.%) deep brown sugar tinted crystals have been grown by the Verneuil flame-fusion technique with the addition of MnO_2 to the melt. Parts of the crystals have been reduced by treatment for 3 h at 1450 K in Formier gas (94% N_2, 6% H_2) atmosphere and subsequently quenched to 300 K by dropping them into a batch of silicone oil. STO:Mn ceramics, about 96–97% of the theoretical x-ray density, were prepared with addition of 0.1%–3% of Mn oxides or $MnSO_4$ with equivalent deficits of Sr or Ti keeping the ratio $(Sr + Mn)/Ti = 1$ or $(Ti + Mn)/Sr = 1$ (A- and B-type ceramics, respectively) as it was described in [7–10]. Sintered materials have been characterized using x-ray, EPR and micro-Raman techniques. As a result, EPR inspection of all our specimens under study reveals the presence of octahedral Mn^{2+} and Mn^{4+} centres and some quantity of Mn oxide nanoparticles [11]. The XRD measurements were performed at room temperature (RT) with a conventional x-ray diffractometer in the Bragg–Brentano configuration using Cu Kα filtered radiation. The analysis has shown well formed cubic perovskite structure. As an example, figure 1 presents an x-ray diffractogram evidencing cubic perovskite structure of STO:Mn(0.1%) B-type ceramics with a lattice parameter $\alpha \sim 3.9005$ Å.

Supplementary Raman spectra measurements have been performed in the 200–1800 cm^{-1} spectral range using a RENISHAW RM 1000 micro-Raman spectrometer with the 514.5 nm line of an Ar^+ laser beam as the excitation source. The obtained RT spectra evidenced the well known second-order scattering inherent to cubic STO [12] together with weak features of the presence of Mn oxide microphases. For example, figure 2 presents RT micro-Raman spectra of STO:Mn(0.1 at.%.) crystals and B-type ceramics for the 550–800 cm^{-1} spectral region. It can be seen that together with 626 cm^{-1} (TO_4–TA; TO_4–TO_1), 684 cm^{-1} ($2TO_3$) and 719 cm^{-1} ($TO_4 + TO_2$) scattering lines conventionally attributed to STO, the weak features of the MnO and MnO_2 Raman spectra [13, 14] centred at 654 and 793 cm^{-1} present too.

The complex dielectric permittivity $\varepsilon' + i\varepsilon''$ was measured under an ac field of ~30 V cm^{-1} in the 100 Hz–1 MHz frequency region with a 4192 LF Hewlett-Packard Impedance Analyzer assembled with a He-flow cryostat allowing temperature cycling within 7–300 K with a rate ±(10–50) mK s^{-1}. Pt–Au electrodes were evaporated onto opposite faces of thin STO:Mn condenser platelets. Far IR reflectivity measurements were performed with a Bruker IFS 113v spectrometer in the 20–2000 cm^{-1} spectral region at RT and $T = 5$ K. The obtained spectra were fitted using a factorized form of the dielectric function [15]. The reflectivity spectrum fitted by the factorized oscillator model and the complex permittivity was calculated as

$$\varepsilon^*(\omega) = \varepsilon_\infty \prod_{j=1}^{n} \frac{\omega_{\mathrm{LO}j}^2 - \omega^2 + i\omega\gamma_{\mathrm{LO}j}}{\omega_{\mathrm{TO}j}^2 - \omega^2 + i\omega\gamma_{\mathrm{TO}j}};$$

$$R(\omega) = \left| \frac{\sqrt{\varepsilon^*(\omega)} - 1}{\sqrt{\varepsilon^*(\omega)} + 1} \right|^2,$$

where $\omega_{\mathrm{TO}j}$ and $\omega_{\mathrm{LO}j}$ are transverse and longitudinal frequencies, $\gamma_{\mathrm{TO}j}$ and $\gamma_{\mathrm{LO}j}$ are the corresponding damping constants, ε_∞ is the optical permittivity.

3. Results and discussion

Figure 3 presents the temperature dependence of the low frequency permittivity taken at different selected frequencies for STO:Mn crystals. The inset shows the respective loss behaviour. It can be seen that magnitude of the permittivity

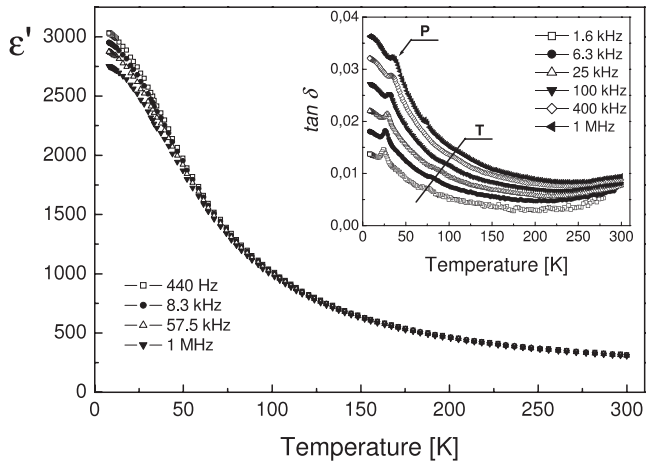

Figure 3. Dielectric permittivity and losses in $SrTiO_3$:Mn(0.1 at.%) crystals.

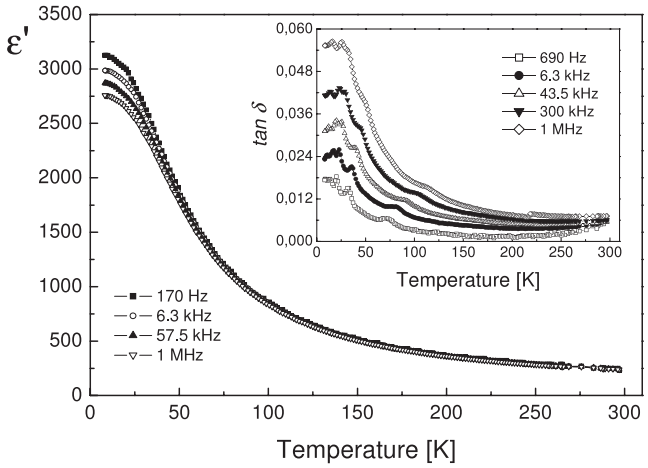

Figure 4. Dielectric permittivity and losses in $SrTiO_3$:Mn(0.1 at.%) B-type ceramics.

at RT is ∼315 which is actually the same as for nominally pure STO crystals $\varepsilon' \sim 307$ [16]. Practically nondispersive permittivity rises on cooling but not as strongly as in nominally pure crystals reaching only ∼3000 at $T = 7$ K (∼18 000 in randomly oriented nominally pure STO single crystals [17]).

Such depressing of the low temperature magnitude of the permittivity can signify Mn impurity induced evolution of the dielectric behaviour from the quantum paraelectric and/or sample inhomogeneity [18, 19]. A weak dielectric dispersion emerges in the real part of the permittivity at low temperatures which is more distinctly seen in losses (inset of figure 3). There two relaxations can be distinguished: P-relaxation in the 21–38 K temperature region and faintly pronounced T-relaxation in the 76–114 K region. It was found that both relaxations obey the Arrhenius law with $\tau_0 \sim 5 \times 10^{-13}$ s, $U = 40$ meV, and $\tau_0 \sim 7 \times 10^{-13}$ s and $U = 120$ meV values, respectively. Note that parameters obtained for the P-relaxation appeared to be similar to those reported in [5, 6] and were connected to Mn^{2+}_{Ti}–O^- or O^-–Mn^{2+}_{Ti}–O^- polaronic-type related centres.

Figure 4 presents the temperature dependence of the dielectric permittivity and losses for B-type ceramics with the same doping degree (0.1 at.%) as for STO:Mn crystals.

Surprisingly, the dielectric permittivity of the B-type ceramics appeared to be very close in magnitude and temperature behaviour to that in STO:Mn(0.1 at.%) crystals. The magnitude of the permittivity is $\varepsilon' \sim 245$ at RT and rises on cooling down up to $\varepsilon' \sim 3000$ at $T = 7$ K too, as in crystals. The effect is clearly illustrated in figure 5 which presents the temperature behaviour of the dielectric permittivity and respective Curie–Weiss plots (see the inset in figure 5), taken at 1.2 kHz for 0.1 at.% Mn doped STO crystal and B-type ceramics.

Analysis has shown that the temperature behaviour of the permittivity in STO:Mn(0.1 at.%.) crystals obeys well the Barrett formula [20]

$$\varepsilon'(T) = A + \frac{C}{T_s \coth(T_s/2T) - T_0},$$

where $T_s = T_1/2 = h\omega_{zp}/2k$ is the quantum fluctuation strength, $T_1 = 94$ K, $T_0 = 16.5$ K is the 'high temperature'

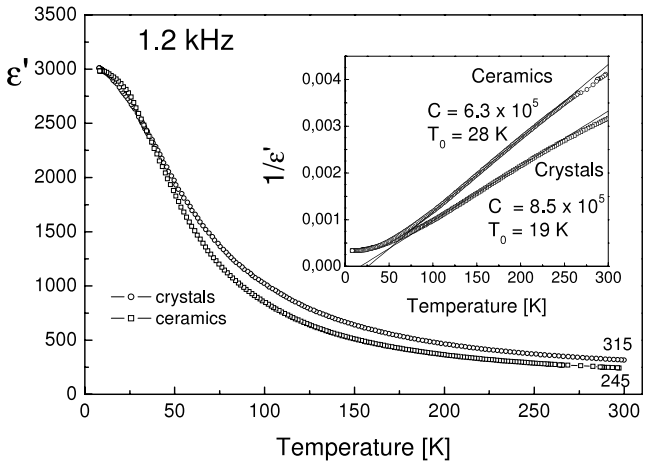

Figure 5. Dielectric permittivity of $SrTiO_3$:Mn(0.1 at.%) B-type ceramics and $SrTiO_3$:Mn(0.1 at.%) crystals. The inset shows the Curie–Weiss fits ($\varepsilon' = C/(T - T_0)$).

Curie–Weiss temperature ($T_1 = 84$ K and $T_0 = 38$ K, respectively, for nominally pure STO crystals [2]).

It is well known that depressing of permittivity at low temperatures in ceramics with respect to crystals is a characteristic property of ceramics and granular materials due their inhomogeneity, the effect of grains, grain boundaries, etc [18, 19]. Using such logic we come to the suggestion that the obtained result (very close temperature behaviour and magnitudes of permittivity in 0.1 at.% Mn doped B-type ceramics and crystals) evidences inhomogeneity of weakly concentrated STO:Mn crystals too. In this case it is necessary very carefully to use Curie–Weiss and Barrett fits parameters obtained for STO:Mn crystals and ceramics, as in all inhomogeneous materials.

Both in STO:Mn(0.1 at.%) crystals and in STO:Mn (0.1 at.%) B-type ceramics, dielectric relaxation is not clearly visible in the real part of the permittivity. However, in losses at least four pronounced Arrhenius-type dielectric relaxations in ceramics can be distinguished in the 8–15 K ($\tau_0 \sim 9 \times 10^{-12}$ s,

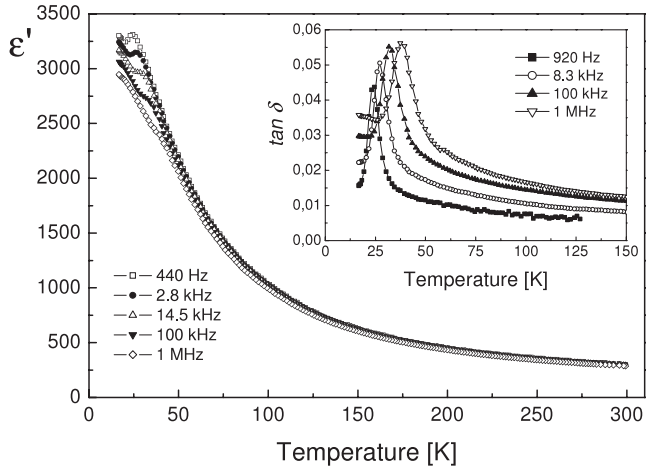

Figure 6. Dielectric permittivity and losses in $SrTiO_3$:Mn(0.1 at.%) reduced crystals.

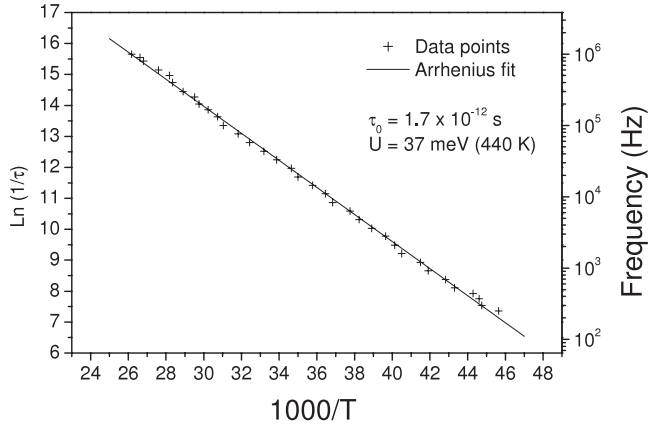

Figure 7. Arrhenius plot for reduced $SrTiO_3$:Mn(0.1 at.%) crystals. The plot was constructed from tan $\delta(T)$ maxima positions taken at different selected frequencies.

$U = 13$ meV), 20–30 K ($\tau_0 \sim 1.7 \times 10^{-13}$ s, $U = 36$ meV), 30–40 K ($\tau_0 \sim 3.2 \times 10^{-11}$ s, $U = 43$ meV) and 67–125 K ($\tau_0 \sim 9 \times 10^{-13}$ s, $U = 120$ meV) temperature regions (see the inset in figure 4). It can be seen that P- and T-relaxations inherent to STO:Mn(0.1 at.%) crystals present in STO:Mn(0.1 at.%) B-type ceramics as well. The nature of the lowest in energy relaxation needs further investigation. For P- and T-relaxations the following interpretation is suggested. In agreement with [5, 6], taking into account the characteristic value of the activation energy (∼40 meV), P-relaxation can be attributed to dipole reorienting centres connected to Mn^{2+} and O^- related polarons. A contribution of the relaxation of Mn^{4+} off-centres in Ti^{4+} sites has to be excluded since in actual cases the off-centre position of Mn^{4+} in Ti sites itself is not too obvious. Besides, in spite of the ionic radius $r^{4+}_{Mn} \sim 0.53$ Å being smaller than $r^{4+}_{Ti} \sim 0.65$ Å [21] such off-centre related polar reorientations have to be of the same order as for Li^+ off-centre reorientation in $KTaO_3$, i.e. having activation energy ∼86–90 meV [22]. Moreover, in the past dielectric experiments, relaxation connected with Ti^{4+} off-centre reorientations revealed as provided by La co-doping of STO:Mn ceramics only with dispersion displaying at ∼170 K [23]. The nature of the T-relaxation with activation energy ∼120 meV can be connected with $O^1_h - D^{18}_{4h}$ structural transition related effects.

In the case of polaronic scenarios the low temperature P-relaxation should strongly depend on the concentration of Mn^{2+} centres and oxygen vacancies, which increases with reduction [24].

Our experiments confirm this statement. Figure 6 shows the temperature dependence of the dielectric permittivity taken at different selected frequencies for STO:Mn(0.1 at.%) reduced crystals. It can be seen that reduction is indeed accompanied by the emergence of the low temperature dielectric relaxation already in the real part of the dielectric permittivity. This relaxation appeared to be P-relaxation brightly displaying in losses (see the inset in figure 6) obeying well the Arrhenius law with parameters $\tau_0 \sim 1.7 \times 10^{-12}$ s and $U = 37$ meV (see figure 7).

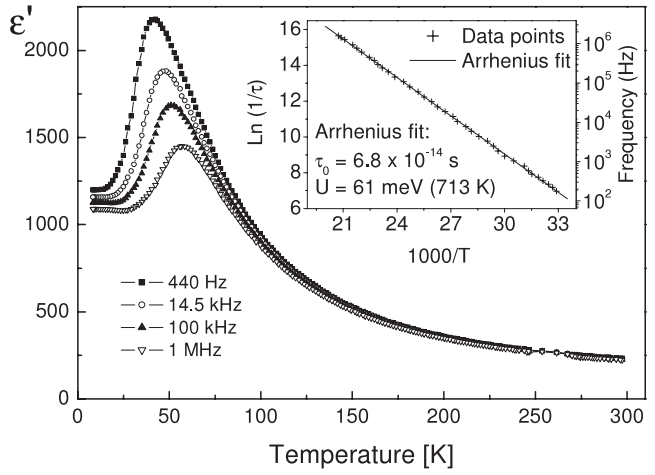

Figure 8. Dielectric permittivity for $SrTiO_3$:Mn(1 at.%) B-type ceramics. The inset shows the Arrhenius plot constructed from tan $\delta(T)$ maxima positions taken at different selected frequencies.

So we conclude that the reorientations of Mn^{2+}_{Ti}–O^- or O^-–Mn^{2+}_{Ti}–O^- polaronic-type related centres in low temperature dielectric relaxation in weakly doped STO:Mn(0.1 at.%) and STO:Mn(0.1 at.%) B-type ceramics play the dominating role. Regarding T-relaxation, it is not seen in figure 6. It can be tentatively related to competitive losses increasing in the reduced STO:Mn(0.1 at.%) crystals, where T-relaxation appeared to be hidden.

Let us consider dielectric properties of more heavily Mn doped A- and B-type STO ceramics. Figures 8 and 9 present temperature dependences of dielectric permittivity taken at different selected frequencies for STO:Mn(1 at.%) B-type and STO:Mn(1 at.%) A-type ceramics. It can be seen that both ceramics exhibit brightly pronounced dielectric relaxation. The insets of figures 8 and 9 show that these relaxations obey well the Arrhenius law with nearly the same parameters $\tau_0 \sim 6.8 \times 10^{-14}$ s and $U = 61$ meV in B-type and $\tau_0 \sim 9.2 \times 10^{-15}$ s and $U = 63$ meV in A-type ceramics, respectively. Experiments performed with more heavily Mn(2–3 at.%) concentrated

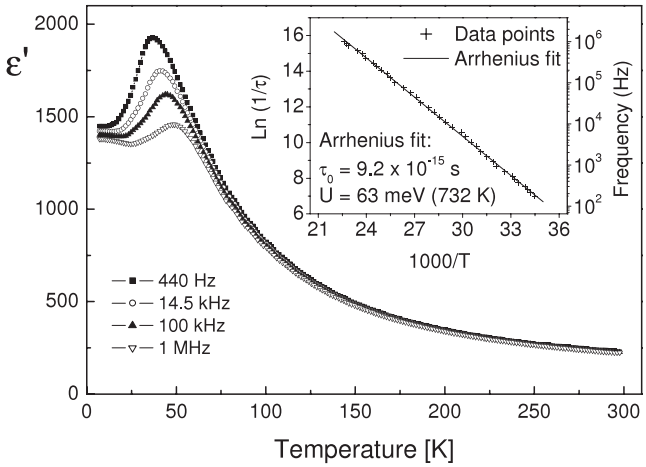

Figure 9. Dielectric permittivity for $SrTiO_3$:Mn(1 at.%) A-type ceramics. The inset shows the Arrhenius plot constructed from $\tan\delta(T)$ maxima positions taken at different selected frequencies.

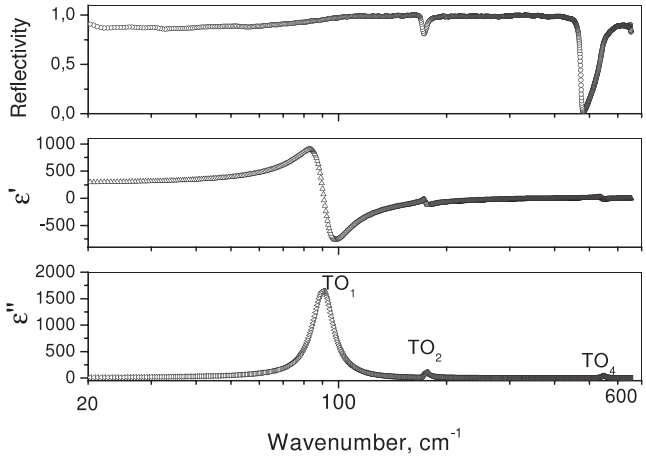

Figure 10. FTIR reflectivity spectra at RT in $SrTiO_3$:Mn(0.1 at.%) crystals. Real and imaginary parts of the dielectric permittivity are calculated from the IR reflectivity fit.

B-type and A-type ceramics reveal similar relaxations with very close activation energies ∼59–68 meV (depending on Mn concentration). This activation energy sufficiently differs from that for weakly concentrated STO:Mn(0.1 at.%) crystals and STO(0.1 at.%) B-type ceramics (∼40 meV) described above.

It seems this relaxation is caused by increased inhomogeneity of rather heavily Mn doped STO ceramics in which, according to [11], Mn distributes inhomogeneously accumulating at the grain boundaries. In weakly doped STO:Mn ceramics this effect is much less pronounced and dielectric relaxation is mostly caused by polaronic related reorientations mentioned above. Thus, our results disagree with observations and conclusions [7–10] where dielectric dispersion and low temperature polar behaviour were found only in SMT compositions considered as $Sr_{1-x}Mn_xTiO_3$ (SMT) ceramics with Mn^{2+} off-centre substituted Sr sites.

At last, a suggestion about heterogeneity of STO:Mn (0.1 at.%) crystals following from dielectric measurements, has found additional proof in FTIR experiments. Figure 10 presents an IR reflectivity spectrum collected at RT for

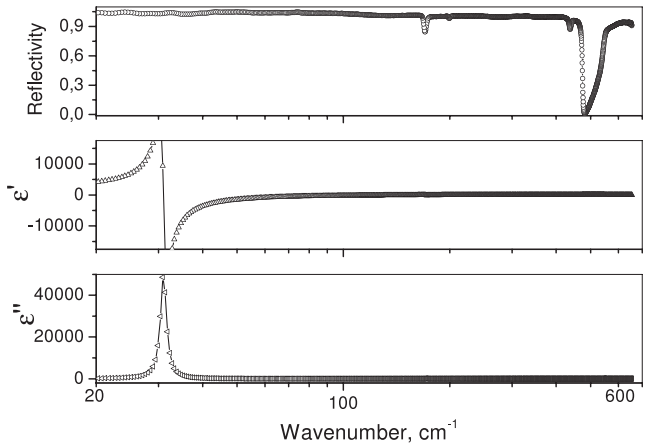

Figure 11. FTIR reflectivity spectra at $T = 5$ K in $SrTiO_3$:Mn(0.1 at.%) crystals. Real and imaginary parts of the dielectric permittivity are calculated from the IR reflectivity fit.

STO:Mn(0.1 at.%) crystals and spectra of the real and imaginary parts of dielectric permittivity calculated from the IR reflectivity fit. It can be seen that the TO_1 phonon contribution provides the magnitude of the real part of the low frequency dielectric permittivity $\varepsilon' \sim 300$, which agrees well with that obtained from a direct dielectric permittivity experiment (315).

Figure 11 shows that the same IR reflectivity data were taken at $T = 5$ K. It can be seen that in contrast to the RT case, where IR reflectivity describes well the magnitude of the low frequency permittivity, IR reflectivity and phonon modes contribution provide at least $\varepsilon' \sim 4000$ for low frequency permittivity at $T = 5$ K, whereas direct dielectric measurements yield $\varepsilon' \sim 3000$. This also proves inhomogeneity of STO:Mn(0.1 at.%) crystals whose experimental low temperature permittivity appeared to be an 'effective one', being depressed as for grainy systems.

4. Conclusions

The low frequency dielectric permittivity (100 Hz–1 MHz) study supplemented with IR reflectivity and micro-Raman experiments has been performed on a series of $SrTiO_3$:Mn(0.1–3 at.%) A- and B-type ceramics (sintered with deficit of Sr or Ti, maintaining the ratios (Sr + Mn)/Ti and (Ti + Mn)/Sr = 1, respectively). The results obtained are compared with the first dielectric spectroscopy studies of STO:Mn(0.1 at.%) single crystals. Surprisingly, STO:Mn(0.1 at.%) crystals and STO:Mn(0.1 at.%) B-type ceramics reveal nearly the same magnitude and temperature dependence of the dielectric permittivity. The practically nondispersive permittivity rises on cooling and reaches ∼3000 at $T = 7$ K in both materials. At the same time IR reflectivity evidences that the TO phonon contribution provides a magnitude of the low temperature permittivity of at least $\varepsilon' \sim 4000$ at $T = 5$ K. Because depressing of permittivity magnitude at low temperature in ceramics with respect to crystals is a characteristic property of ceramics and granular materials [18, 19], both observed features were understood as evidence of STO:Mn(0.1 at.%) crystal inhomogeneity. Both weakly doped STO:Mn(0.1 at.%) crystals and

STO:Mn(0.1 at.%) B-type ceramics reveal at least two faint low temperature relaxations with Arrhenius activation energies ∼37–40 meV and ∼120–130 meV (P- and T-relaxations, respectively). These relaxations can be seen in losses only and as in [5, 6] are tentatively attributed to reorientation of defects associated with Mn^{2+}_{Ti}–O^- or O^-–Mn^{2+}_{Ti}–O^- related polaronic centres and O^1_h–D^{18}_{4h} structural transition related effects, respectively. P-relaxation strongly enhances in reduced STO:Mn(0.1 at.%) crystals and becomes distinctly pronounced in the real part of the permittivity. Because according to EPR studies [24, 11] reduction is accompanied by increasing of Mn^{2+}_{Ti}–V_0 axial centre concentration, this confirms the polaronic related nature of the P-relaxation. Our findings agree well with the results of EPR studies [11] performed on the samples used in the presented work. It was found that both crystals and ceramics evidenced pronounced inhomogeneity in Mn centre distribution. Mn occurs as isotropic cubic Mn^{2+} and Mn^{4+} centres and large parts of them form Mn oxide enriched nanoregions.

More heavily Mn doped ceramics revealed strongly pronounced low temperature dielectric relaxation as in A-type as in B-type compositions. This relaxation appeared to be nearly the same in the two types of ceramics having the Arrhenius activation energy ∼59–68 meV (depending on Mn concentration). Our observations contradict the results and suggestions of [7–10] that low temperature relaxation is present in STO:Mn(0.1% at) A-type ceramics only and caused by Mn^{2+}(Sr) off-centre related reorientations. To our mind EPR investigations reported in [9, 25] did not present cogent evidence and arguments and cannot be considered as giving proof of the presence of such Mn^{2+} off-centres. The existence of Mn^{2+}(Sr) off-centres and related reorientations is doubtful and has to be studied further in more detail. At least our and the EPR [11] studies of STO:Mn crystals and ceramics did not support this point of view. Our results with weakly concentrated STO:Mn(0.1 at.%) ceramics and crystals agree with the suggestion of [5, 6] about a polaronic related nature of the low temperature relaxation in STO:Mn. The nature of the dielectric relaxation in more heavily Mn concentrated ceramics is tentatively attributed to processes taking place at grain boundaries and manganese oxide enriched nanoregions evidenced in [4, 11]. Further dielectric permittivity studies in a wider frequency region and respective analysis should provide valuable data concerning the nature of the actual dielectric relaxations, e.g. relaxation type and relaxation time distribution. This separate work is in progress and will be published elsewhere. Special attention will be paid to details of Mn centre structure and attempts to grow and study perfect STO crystals with homogeneous distribution of Mn centres.

Acknowledgments

This work was supported by Grants RFBR 06-02-17320, Sc. Sc. 5169.2006.2, KAN 301370701, KJB100100703 and 1QS100100563 of AV ČR, 1M06002 MŠMT ČR.

References

[1] Rodrigues R, Ellis D E and Dravid V P 1999 *J. Am. Ceram. Soc.* **82** 2395
[2] Zhang Q 2004 *J. Phys. D: Appl. Phys.* **37** 98
[3] Norton D P, Theodoropoulou N A, Herbard A F, Budal J D, Boatner L A, Pearton S J and Wolson R G 2003 *Electrochem. Solid-State Lett.* **6** G 19
[4] Azzoni C B, Mozzati M C, Galinetto P, Paleari A, Masarotti V, Bini M and Gapsoni D 2000 *Solid State Commun.* **114** 617
[5] Lemanov V V, Smirnova E P, Sotnikov A V and Weihnacht M 2004 *Phys. Solid State* **46** 1442
[6] Lemanov V V, Sotnikov A V, Smirnova E P and Weihnacht M 2005 *J. Appl. Phys.* **98** 056102
[7] Tkach A, Vilarinho P M and Kholkin A L 2005 *Acta Mater.* **53** 5061
[8] Tkach A, Vilarinho P M and Kholkin A L 2005 *Appl. Phys. Lett.* **86** 172902
[9] Tkach A, Vilarinho P M and Kholkin A L 2006 *Acta Mater.* **54** 5385
[10] Tkach A, Vilarinho P M, Kholkin A L, Pashkin A, Veljko A and Petzelt J 2006 *Phys. Rev.* B **73** 104113
[11] Badalyan A G, Azzoni C B, Galinetto P, Mozzati M C, Trepakov V A, Savinov M, Deyneka A, Jastrabik L and Rosa J 2007 *J. Phys.: Conf. Ser.* **93** 012012
[12] Nilsen W G and Scinner J G 1968 *J. Chem. Phys.* **48** 2250
[13] Buciuman F, Patcas F, Craciun R and Zahn D R T 1999 *Phys. Chem. Phys.* **1** 185
[14] Bernard M-C, Golf A H-L, Thi B V and de Torres S C 1993 *J. Electrochem. Soc.* **140** 3065
[15] Gevrais F 1983 *Infrared and Millimeter Waves* vol 8, ed K J Button (New York: Academic) (High-Temperature Infrared Reflectivity Spectroscopy by Scanning Interferometry) Chapter 7, p 279
[16] Samara G A and Giardini A A 1965 *Phys. Rev.* B **140** A954
[17] Graenicher H 1956 *Helv. Phys. Acta.* **29** 210
[18] Rychestky I and Petzelt J 2004 *Ferroelectrics* **303** 137
[19] Petzelt J, Ostapchuk T, Gregora I, Savinov M, Chvostova D, Kiu J and Shen Zh 2006 *J. Eur. Ceram. Soc.* **26** 2855
[20] Barrett J H 1952 *Phys. Rev.* B **86** 118
[21] Shannon R D 1976 *Acta Crystallogr.* A **32** 751
[22] Höchli U T, Knorr K and Loidl A 1990 *Adv. Phys.* **39** 405
[23] Skanavi G I, Ksendzov O M, Trigubenko V A and Pokotilov V G 1958 *Sov. Phys.—JETP* **6** 250
[24] Blazey K W, Cabrera J M and Müller K A 1983 *Solid State Commun.* **45** No 10 903
[25] Laguta V V, Kondakova I P, Bykov I P, Glinchuk M D, Vilarinho P M, Tkach A and Jastrabik L 2007 *Phys. Rev.* B **76** 054104